

## Mechanical Behavior of Nanocrystalline NaCl Islands on Cu(111)

Ch. Bombis,<sup>1</sup> F. Ample,<sup>3</sup> J. Mielke,<sup>1,2</sup> M. Mannsberger,<sup>1</sup> C. J. Villagómez,<sup>1,2</sup> Ch. Roth,<sup>1</sup> C. Joachim,<sup>3</sup> and L. Grill<sup>1,2,\*</sup>

<sup>1</sup>*Physics Department, Freie Universität Berlin, Arnimallee 14, 14195 Berlin, Germany*

<sup>2</sup>*Fritz-Haber-Institut of the Max-Planck Society, Faradayweg 4-6, 14195 Berlin, Germany*

<sup>3</sup>*CEMES-CNRS, 29 rue J. Marvig, 31055 Toulouse Cedex, France*

(Received 10 March 2010; published 4 May 2010)

The mechanical response of ultrathin NaCl crystallites of nanometer dimensions upon manipulation with the tip of a scanning tunneling microscope (STM) is investigated, expanding STM manipulation to various nanostructuring modes of inorganic materials as cutting, moving, and cracking. In the light of theoretical calculations, our results reveal that atomic-scale NaCl islands can behave elastically and follow a classical Hooke's law. When the elastic limit of the nanocrystallites is reached, the STM tip induces atomic dislocations and consequently the regime of plastic deformation is entered. Our methodology is paving the way to understand the mechanical behavior and properties of other nanoscale materials.

DOI: [10.1103/PhysRevLett.104.185502](https://doi.org/10.1103/PhysRevLett.104.185502)

PACS numbers: 62.25.-g, 68.37.Ef, 81.07.Bc, 81.40.Jj

The mechanical response of crystals on external stress ranges from elastic bending, preserving their stability, to permanent deformation due to nucleation of atomic defects and dislocations [1,2]. Various crystalline materials and thin films with dimensions from the macroscopic to the scale of hundreds or several tens nanometers have been studied in terms of mechanical properties [3–7]. Down at the atomic scale, theoretical studies addressed structural transitions [8] and cleaving [9] of a few layers of crystalline NaCl. Nanofriction of alkali halides was studied theoretically [10] and by atomic force microscopy (AFM) [11,12], but no structuring and strain deformation have been demonstrated so far. The scanning tunneling microscope (STM) is a powerful tool for the lateral manipulation of matter at the atomic scale [13–16], but has also been used for the displacement of larger objects as Ag nanoparticles [17], Au nanoislands [18], large C<sub>60</sub> islands [19], or organic crystallites [20] on surfaces.

In this Letter, nanostructuring of NaCl crystallites on a copper substrate by STM manipulation is presented in combination with molecular mechanics calculations, revealing details about their mechanical properties under external stress. Experiments were performed in ultrahigh vacuum (base pressure of 10<sup>-10</sup> mbar) with a low temperature STM (Createc) at 9 K. The tungsten tip is presumably covered with copper because of routine tip crashes to improve its quality. Imaging was performed in the constant-current mode, bias voltages are applied to the sample.

NaCl grows crystalline in a homogeneous manner on differently oriented single-crystal Cu surfaces [21–23]. After NaCl (99.999% purity; Sigma-Aldrich) deposition on a slightly cooled substrate (270–280 K), NaCl islands of different height are found on clean Cu(111) [Fig. 1(a)]. Mainly bilayer islands are present, but due to the cold substrate [22] we observe also small monolayer areas. Atomic resolution images of the (001) oriented NaCl film [Fig. 1(b)] show that straight step edges are formed along nonpolar directions of the NaCl crystallites. A high density

of kinks causes a dendritelike shape of the bilayer islands. This particular crystallite shape is a key property for our nanostructuring experiments. When the STM tip is approached laterally towards a NaCl crystallite on Cu(111), the island can respond in various ways to the applied force [Fig. 1(c)]. If the diffusion barrier  $E_{\text{diff}}$  of the crystallite—determined by the NaCl island area—is rather high, the tip locally removes Na and Cl atoms in a cuttinglike procedure. On the other hand, the entire island can move on the surface if  $E_{\text{diff}}$  is smaller than the local interatomic Na-Cl bond  $E_{\text{Na-Cl}}$  at the position of tip approach (the calculated energy required to remove one atom from the NaCl bilayer is 0.23 eV). Figures 1(d) and 1(e) demonstrate cutting of a bilayer of a large NaCl island with the STM tip. After manipulation [Fig. 1(e)] a narrow channel in the NaCl layer and the additional material, removed from the bilayer during the cutting, is visible at the end of the tip pathway (lower right corner). This “snowplough” behavior can be explained by the rather weak interaction of NaCl with the metallic tip; i.e., the removed material hardly sticks on the STM tip. NaCl crystallites of smaller size are moved on the surface upon manipulation. The diffusion barrier increases with the island size, similar to the manipulation of fullerene islands [19], as only NaCl islands smaller than 250 nm<sup>2</sup> in size can be rotated and displaced on the surface independent of their relative orientation. Figures 2(a) and 2(b) show an example of the controlled dislocation of a comparatively large island. Lateral movement can be induced either by dragging or pushing, approaching the tip above the island or above the copper surface, respectively [Fig. 2(c)]. Defects are often observed at the tip contact point after manipulation, because in both modes a mechanical contact between tip apex and nanoisland is established. Note that a NaCl island can even be manipulated up and down a Cu(111) step edge without losing its crystallinity.

In addition to moving and cutting of nanoislands, the intermediate case of cracking [Fig. 1(c)] occurs if a narrow,

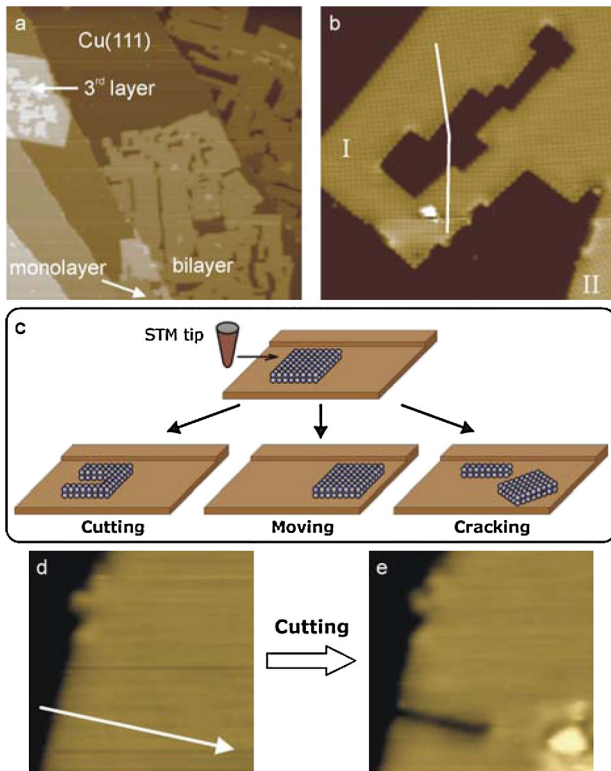


FIG. 1 (color online). (a) STM image ( $I_T = 0.31$  nA,  $U_T = -1$  V,  $175 \times 175$  nm<sup>2</sup>) of (001) oriented NaCl islands partially covering the Cu(111) surface. (b) Atomic resolution STM image ( $I_T = 0.31$  nA,  $U_T = -1$  V,  $22 \times 22$  nm<sup>2</sup>) of a bilayer NaCl island. Note that domain I is laterally compressed and rotated with respect to domain II. (c) Scheme of the three possible processes that can occur when an STM tip is approached laterally towards a NaCl nanocrystallite. (d),(e) STM images ( $I_T = 0.31$  nA,  $U_T = -1$  V,  $10 \times 10$  nm<sup>2</sup>) of the same area before (d) and after (e) cutting the NaCl crystallite by lateral manipulation with the tip in constant-current mode ( $I_T = 100$  nA,  $U_T = -0.05$  V).

long NaCl bilayer is fixed at one end [Figs. 2(d)–2(g)]. If such a cantilever is manipulated in a pushing mode perpendicular to its long axis, a piece is cracked off [Figs. 2(d) and 2(e)]. Note that the island does not break at the pathway of the tip, but the cracking edge is always shifted parallel from it [dashed lines in Figs. 2(d) and 2(f)]. After moving the cracked piece laterally, another piece of the same cantilever is cracked [Figs. 2(f) and 2(g)]. The cracked cantilever pieces in Fig. 2(g) have approximately the same size. To understand this behavior, molecular mechanics calculations were performed, keeping two columns of atoms at one edge (left edge of the corresponding images) fixed (Fig. 3). The simulations were done using a modified version of the ASE+ program [24] to accommodate the ionic character of the bonding in the NaCl material. The Cu surface is considered in the calculations, but not plotted in Fig. 3 for the sake of clarity.

The resulting length  $x_2$  of the cracked NaCl crystallite is plotted in Fig. 3(b) as a function of the cantilever length for

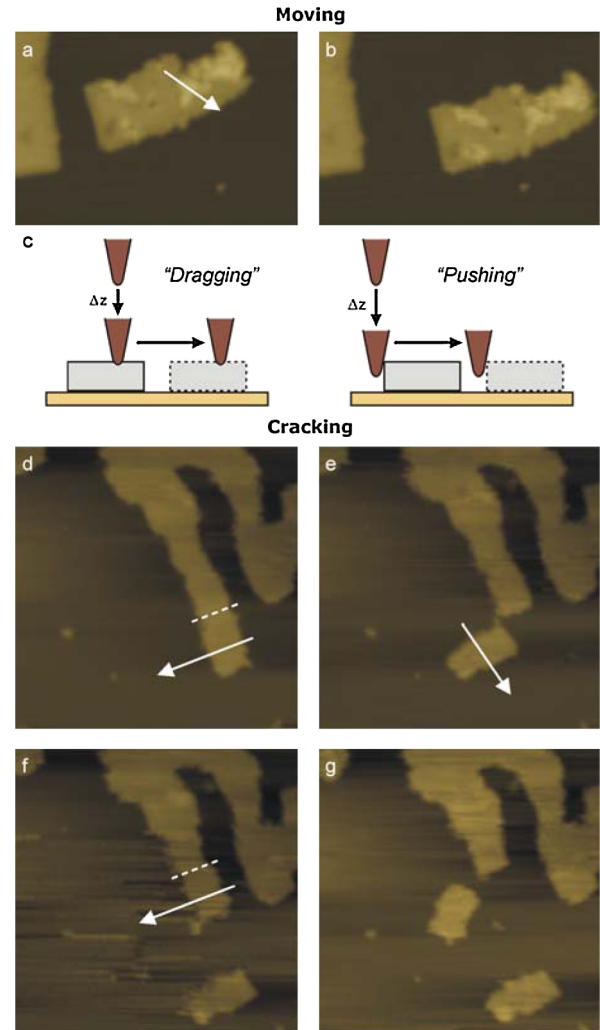


FIG. 2 (color online). (a),(b) STM images ( $I_T = 0.31$  nA,  $U_T = -1$  V,  $30 \times 44$  nm<sup>2</sup>) before and after the motion of a NaCl nanoisland upon lateral manipulation. (c) Schemes of the two manipulation modes used for the dislocation of NaCl islands. (d)–(g) STM images ( $I_T = 0.31$  nA,  $U_T = -1$  V,  $44 \times 44$  nm<sup>2</sup>) of the same surface area before (d),(f) and after (e),(g) two cracking experiments in the upper and lower panel, respectively. Lateral manipulation is done in these experiments in the constant height mode using a bias voltage of  $-0.05$  V ( $z$  offset =  $7$  Å for dragging or  $4$  Å for pushing, manipulation speed is  $10$  Å/s).

different widths  $y$ . For very short cantilevers (small  $x_1$  values),  $x_2$  obviously increases linearly for all cases, because the cantilever breaks at the fixed end (in agreement with similar experiments) and  $x_1 = x_2 + x_3$ . For longer cantilevers  $x_2$  reaches constant values, which are larger for wider cantilevers, meaning that the cracking point of a cantilever is given by its width and does not depend on its length. The copper surface has no influence on the cracking point, due to weak physisorption. The reason for this behavior, similar to macroscopic cracking, is obtained from the calculated atomic displacements within the cantilever during cracking [Fig. 3(c)]. After applying sufficient force

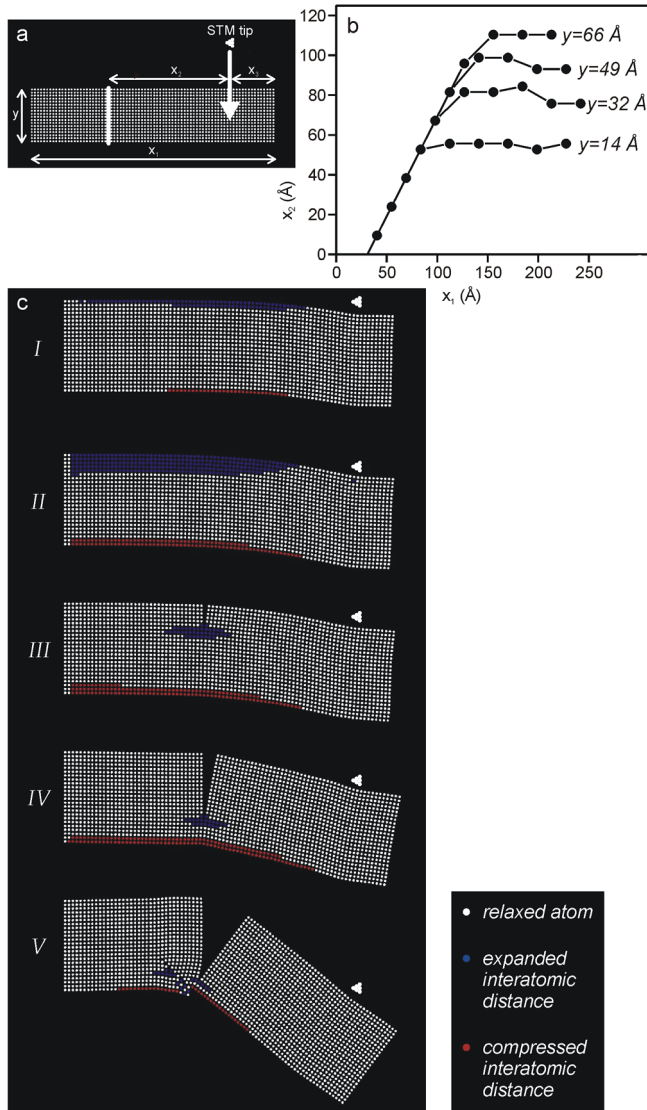


FIG. 3 (color online). (a) Length and width of a nanoisland, which is fixed at the left edge, are defined by  $x_1$  and  $y$ . The STM tip, its pathway (arrow) and the cracking line are shown, whereas  $x_2$  is the distance between tip and cracking edge. (b) Calculated lengths  $x_2$  of cracked crystallites [ $24 \times 85$  NaCl pairs arranged vertically in two atomic layers adsorbed on Cu(111)] as a function of the cantilever dimensions  $x_1$  for different widths  $y$  ( $x_3$  is kept constant at  $31 \text{ \AA}$ ). (c) Sequence of the cracking process for 5 particular time intervals named I–V, visualizing the spatial distribution of the strain within the islands. Atoms in white are in their initial, relaxed position, while the colored ones correspond to expanded and compressed interatomic distances in the  $x$  direction with a difference larger than  $0.02 \text{ \AA}$  as compared to the initial distances.

to the cantilever, it is elastically deformed and the interatomic distances are modified. Situation II in Fig. 3(c) represents the moment right before cracking and thus the maximum elastic deformation, which is in macroscopic material science called the “elastic limit.” It can be clearly seen how elastic strain is created in the cantilever not at the tip contact point, but at a distance of about  $x_2$  from it.

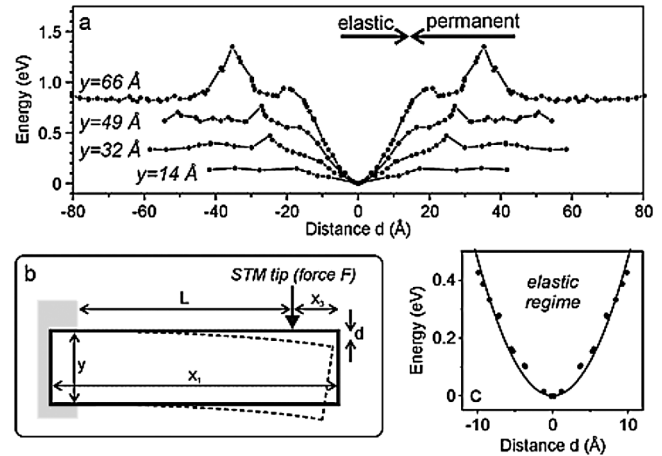


FIG. 4. (a) Total energy as a function of the deformation distance  $d$  for NaCl cantilever of  $229 \text{ \AA}$  in length and various widths  $y$ . The arrows mark the regimes of elastic and permanent deformation of the cantilever for the  $y = 66 \text{ \AA}$  curve. (b) Schematic top view of a NaCl bilayer during the cracking process. The STM tip is moving from top to the bottom, causing the deformation of the bilayer that is quantified by the distance  $d$  from the initial status. (c) Fitting of the total energy curve for  $y = 66 \text{ \AA}$  with a parabolic function in the regime of elastic deformations.

Consequently, the cantilever breaks at this position (always in a nonpolar direction) and the stress is released immediately afterwards (situation III). This explains why  $x_2$  remains constant for different  $x_3$  values, because elastic strain can only be created towards the fixed cantilever end. When the tip is moved further, the strain is located at the end of the line of fracture and consequently the cracking continues until a NaCl crystallite is separated from the cantilever.

The simulations confirm the experimental observation and reveal that a long NaCl nanocantilever is elastically deformed by the STM tip before cracking. When calculating the total energy of the nanocantilever as a function of the deformation distance  $d$  [Figs. 4(a) and 4(b)], two regimes appear: at weak deformations (small  $d$ ), the solid nanocantilever shows a parabolic mechanical response [see Fig. 4(c)], when it is moderately pushed at the end. This result shows that the atomic-scale cantilever follows Hooke’s law, which describes elasticity in macroscopic mechanics, as it exhibits a mechanical response of  $\frac{1}{2}kd^2$  ( $k$  is the spring constant). The spring constant of the NaCl cantilever is  $0.12 \text{ N/m}$  for  $y = 4.9 \text{ nm}$  [increasing with  $y$  in Fig. 4(a)], which is in the range of AFM cantilevers with macroscopic lengths of several hundred micrometers [25].

The bending  $d$  of a macroscopic cantilever upon application of an external force  $F$  [see Fig. 4(b)], can be calculated from Young’s modulus  $E$  of its material [26]:

$$d = 4 \frac{L^3}{Ey^3} F$$

where  $t$  is the thickness of the layer. This leads to a spring constant of

$$k = \frac{Ey^3t}{4L^3}.$$

We applied this equation to a cantilever of NaCl with dimensions  $L = 190 \text{ \AA}$  and  $y = 49 \text{ \AA}$  and a thickness  $t$  of  $5.64 \text{ \AA}$  (i.e., a bilayer of NaCl). The result is  $k = 0.1 \text{ N/m}$ , which is close to the value calculated by molecular mechanics (see Fig. 4). The material's properties are included in the NaCl Young's modulus of 39.98 GPa. The surprising similarity shows that equations from macroscopic mechanics can thus, although derived for homogeneous media without internal structure, also be applied at the atomic scale. Thus, the elastic behavior of a surface nanocantilever can be described by a classical Hooke's law. Moreover, the elastic character of this deformation regime is apparent if the applied force, i.e., the tip apex, is removed. In this case, the NaCl nanocantilever returns to its original linear shape and thus an elastic back response occurs [from the dashed to the solid shape in Fig. 4(b)]. In the experiments we observed that cantilevers can remain only slightly changed after a manipulation, although a larger deformation should have occurred due to the tip pathway. We conclude that in such a case elastic back response occurs after the cantilever was first bent within the elastic limit and the static situations before and afterwards are imaged by STM. The small changes of the cantilever are in this case presumably due to the interaction with the substrate. Beyond the elastic limit [marked by the two arrows in Fig. 4(a)], elastic strain is released and the nanocantilever cracks. In our simulation, its energy initially increases further, because the detached NaCl nanoisland is compressing the end part of the remaining cantilever [situation V in Fig. 3(c)] before being totally released. When this cracked part is finally pushed away, the total energy remains constant.

The observed classical Hooke's law follows from the collective motion of many displaced NaCl atoms in the nanocantilever. This elastic behavior was found in the simulations for cantilever widths down to only 4 atoms. The potential barrier for local extraction of a single atom from the cantilever (0.23 eV at a deformation distance of a few  $\text{\AA}$ ) is less favorable than the cooperative elastic deformation along the minimum energy reaction pathway [see slopes in the elastic regimes of Fig. 4(a)], which explains the preference of cracking before cutting. This study pro-

vides insight into the elastic deformation and cracking of crystallites at the atomic level and opens new structuring possibilities. Tailored inorganic nanocrystallites of predefined dimensions can be created in this way, using either the cutting or the cracking process, and they can finally be manipulated to any chosen location on the substrate.

This work was funded by the integrated project "Pico-inside" of the European Union and the research initiative "Nanoscale functional materials" of the Freie Universität Berlin. Helpful discussions with Jascha Repp and Gerhard Meyer about the NaCl growth are gratefully acknowledged.

---

\*lgr@fhi-berlin.mpg.de

- [1] J. Li *et al.*, *Nature (London)* **418**, 307 (2002).
- [2] C. A. Schuh, J. K. Mason, and A. C. Lund, *Nature Mater.* **4**, 617 (2005).
- [3] M. D. Kriese *et al.*, *Eng. Fract. Mech.* **61**, 1 (1998).
- [4] Z. C. Xia and J. W. Hutchinson, *J. Mech. Phys. Solids* **48**, 1107 (2000).
- [5] Z. Budrovic *et al.*, *Science* **304**, 273 (2004).
- [6] Y. Champion *et al.*, *Science* **300**, 310 (2003).
- [7] B. Wu, A. Heidelberg, and J. J. Boland, *Nature Mater.* **4**, 525 (2005).
- [8] J. P. K. Doye and D. J. Wales, *Phys. Rev. B* **59**, 2292 (1999).
- [9] K. Kendall, C. W. Yong, and W. Smith, *Powder Technol.* **174**, 2 (2007).
- [10] T. Zykova-Timan *et al.*, *Surf. Sci.* **600**, 4395 (2006).
- [11] E. Gnecco, R. Bennewitz, and E. Meyer, *Phys. Rev. Lett.* **88**, 215501 (2002).
- [12] A. Schirmeisen, D. Weiner, and H. Fuchs, *Phys. Rev. Lett.* **97**, 136101 (2006).
- [13] J. A. Stroscio and D. M. Eigler, *Science* **254**, 1319 (1991).
- [14] L. Grill *et al.*, *Nature Nanotech.* **2**, 95 (2007).
- [15] S. Selvanathan *et al.*, *Appl. Phys. A* **93**, 247 (2008).
- [16] L. Grill, *J. Phys. Condens. Matter* **22**, 084023 (2010).
- [17] J. Grobelny *et al.*, *Nanotechnology* **17**, 5519 (2006).
- [18] J. Yang *et al.*, *J. Vac. Sci. Technol. B* **25**, 1694 (2007).
- [19] R. Lüthi *et al.*, *Science* **266**, 1979 (1994).
- [20] K. Hänel *et al.*, *Surf. Sci.* **600**, 2411 (2006).
- [21] R. Bennewitz *et al.*, *Surf. Sci.* **438**, 289 (1999).
- [22] J. Repp and G. Meyer, *Appl. Phys. A* **85**, 399 (2006).
- [23] R. Bennewitz *et al.*, *Phys. Rev. B* **62**, 2074 (2000).
- [24] F. Ample and C. Joachim, *Surf. Sci.* **602**, 1563 (2008).
- [25] T. R. Albrecht *et al.*, *J. Vac. Sci. Technol. A* **8**, 3386 (1990).
- [26] J. H. He *et al.*, *Mater. Sci. Eng. A* **423**, 134 (2006).